AGU PUBLICATIONS

Geophysical Research Letters

RESEARCH LETTER
10.1002/2017GL072611

Key Points:
- Transient rip currents induce offshore tracer transport of 1.2 km/d on a stratified inner shelf
- Without transient rip currents, offshore transport is reduced 95%
- This mechanism may be important in exporting larvae, pathogens, or other tracers to the inner shelf

Correspondence to:
N. Kumar,
nirni@uw.edu

Citation:
Kumar, N. and F. Feddersen (2017), A new offshore transport mechanism for shoreline-released tracer induced by transient rip currents and stratification, *Geophys. Res. Lett.*, *44*, doi:10.1002/2017GL072611.

Received 12 JAN 2017
Accepted 2 MAR 2017
Accepted article online 15 MAR 2017

A new offshore transport mechanism for shoreline-released tracer induced by transient rip currents and stratification

Nirnimesh Kumar[1] **and Falk Feddersen**[2]

[1]Department of Civil and Environmental Engineering, University of Washington, Seattle, Washington, USA, [2]Scripps Institution of Oceanography, La Jolla, California, USA

Abstract Offshore transport from the shoreline across the inner shelf of early-stage larvae and pathogens is poorly understood yet is critical for understanding larval fate and dilution of polluted shoreline water. With a novel coupling of a transient rip current (TRC) generating surf zone model and an ocean circulation model, we show that transient rip currents ejected onto a stratified inner shelf induce a new, previously unconsidered offshore transport pathway. For incident waves and stratification typical for Southern California in the fall, this mechanism subducts surf zone-origin tracers and transports them at least 800 m offshore at 1.2 km/d analogous to subduction at ocean fronts. This mechanism requires both TRCs and stratification. As TRCs are ubiquitous and the inner shelf is often stratified, this mechanism may have an important role in exporting early-stage larvae, pathogens, or other tracers onto the shelf.

Plain Language Summary The principal offshore transport pathway of shoreline-released intertidal larvae and pathogens within 1 km of the coast is still a mystery, motivating this study. Here a new offshore transport pathway for shoreline pollution and shoreline-released intertidal invertebrate larvae from the surf zone to 1 km offshore is presented. This new and intuitive offshore transport pathway will help provide insight to abundance of offshore larvae and marine population connectivity. This transport pathway is induced by transient rip currents (TRCs, episodic offshore flow from the surf zone) and stratification (temperature difference with depth) and leads to offshore advection of 1.2 km/d. The findings are based on a new model that couples TRC generation to a three-dimensional ocean circulation model. Previous models lacked the TRC-generating mechanism and miss this pathway. Without TRCs the offshore transport is only about 5% of that with TRCs. Study findings have implications for marine population connectivity, marine-protected area design, and export of pathogens, contaminants, and nutrients.

1. Introduction

The shoreline is the origin and terminus for intertidal invertebrate larvae [e.g., *Cowen et al.*, 2006; *Pineda et al.*, 2007; *Cowen and Sponaugle*, 2009; *Shanks et al.*, 2010; *Fujimura et al.*, 2014], thus making the nearshore region (within ≈1 km from the shoreline) critical for intertidal ecosystems. The nearshore region consists of the surf zone (from the shoreline to the seaward extent of depth-limited breaking) and the inner shelf (farther offshore to ≈15 m depth) [e.g., *Lentz and Fewings*, 2012]. Water quality in the nearshore is often compromised by pathogens and excessive nutrient supply from terrestrial runoff [e.g., *Halpern et al.*, 2008, 2012; *Boehm et al.*, 2015]. Offshore tracer transport (e.g., pathogens, contaminants, nutrients, larvae, sediment, and heat) across the stratified inner shelf is complex, three dimensional, and poorly understood. For early-stage (passive) intertidal invertebrate larvae [*Scheltema*, 1986] such transport mechanism is important for the overall larval fate and is relevant for understanding population connectivity [*Pineda et al.*, 2007]. Such transport is also important for diluting the shoreline of pathogens [*Boehm*, 2003; *Grant et al.*, 2005; *Hally-Rosendahl et al.*, 2014].

Tracer experiments and modeling on alongshore uniform coasts demonstrate that transient rip currents (TRCs, episodic offshore flows from surf zone) dominate offshore transport from the surf zone onto the inner shelf out to about three surf zone widths (L_{SZ}) offshore from the shoreline [*Hally-Rosendahl et al.*, 2015; *Suanda and Feddersen*, 2015; *Hally-Rosendahl and Feddersen*, 2016; *Kumar and Feddersen*, 2016a, 2016b]. The situation is

similar on rip-channeled bathymetries [*Brown et al.*, 2015]. Farther offshore on the inner shelf, other potential offshore transport mechanisms may be active. For example, wind [e.g., *Connolly et al.*, 2001; *Shanks and Brink*, 2005], eddies [e.g., *Mullaney and Suthers*, 2013], tides [e.g., *Luettich et al.*, 1999], and internal waves [e.g., *Pineda*, 1994; *Wong et al.*, 2012] may be important physical transport drivers on the shelf. Upwelling-induced cross-shelf circulation has been hypothesized to sweep early-stage larvae offshore [*Roughgarden et al.*, 1988; *Connolly et al.*, 2001]. Yet both early- and late-stage larvae were found to remain close (within 4 km) to shore during both upwelling or downwelling [*Shanks and Shearman*, 2009], as overlapping surface and bottom boundary layers shut down inner-shelf circulation [*Austin and Lentz*, 2002]. Most larval models [e.g., *Cowen et al.*, 2006; *Werner et al.*, 2007; *Siegel et al.*, 2008] do not resolve the nearshore (<1 km from shore), and the principal offshore transport pathway across this inner-shelf region is still a mystery.

TRCs are ubiquitous in the surf zone [*Feddersen*, 2014]. However, their effects on the offshore transport of early-stage larvae, pathogens, or other tracers beyond $3L_{SZ}$ on a stratified inner shelf have not been considered. Here a coupled TRC generating surf zone model and 3-D ocean circulation model [*Kumar and Feddersen*, 2016b] (section 2) are used to examine the effects of TRCs and stratification on offshore transport across the inner shelf of a surf zone-released tracer representative of either early-stage larvae or pathogens. For typical waves, TRCs, and stratification, a new offshore transport pathway for tracer is demonstrated that advects tracer $\approx$1 km offshore at 1.2 km/d (section 3). This pathway requires both TRCs and stratification and is analogous to subduction under ocean fronts (section 4). As TRCs are ubiquitous and the inner shelf is often stratified, this offshore transport mechanism may dominate offshore transport of shoreline-released early-stage larvae and surf zone pathogens.

2. Methods

The Coupled Ocean Atmosphere Wave and Sediment Transport (COAWST) modeling system [*Warner et al.*, 2010; *Kumar et al.*, 2012], coupling the SWAN wave model [*Booij et al.*, 1999] and the three-dimensional Regional Ocean Modeling System (ROMS) [*Shchepetkin and McWilliams*, 2005] circulation model, is used here. ROMS solves the wave-averaged Navier Stokes equations with Boussinesq and hydrostatic approximations. COAWST is wave averaged and cannot generate transient rip currents (TRCs), motivating coupling to a wave-resolving, Boussinesq model funwaveC that accurately simulates TRC generation [*Feddersen*, 2014]. This funwaveC-COAWST coupling involves prescribing funwaveC-simulated rotational wave forcing as a depth-uniform body force to ROMS, generating surf zone eddies and TRCs similar to funwaveC [*Kumar and Feddersen*, 2016a].

The model domain is alongshore (y) uniform with cross-shore (x) width of 800 m and alongshore length of 1000 m, with resolutions 1.25 m and 2 m, respectively. Boundary conditions are alongshore periodic. The model cross-shore bathymetric profile h is near planar for $x > -280$ m and concave farther offshore to weaker slope typical for Southern California inner shelf (Figure 1). Normally incident, directionally spread waves (wave height $H_s = 0.95$ m, peak period $T_p = 10$ s, and directional spread of 10°), typical of early fall in Southern California, are prescribed at the offshore boundary ($x = -800$ m, $h = 14$ m). SWAN provides the irrotational wave parameters to ROMS, to estimate the vertically varying Stokes drift and to force wave setup and setdown. ROMS has 10 bathymetry following vertical (z) levels. The ROMS Coriolis parameter $f = 8.09 \times 10^{-5}$ s^{-1} and initial temperature $T = 20°$ at $z = 0$ m with a constant stratification $\partial T/\partial z = 0.25$ °C m^{-1} are typical for the Southern California Bight. Salinity is constant. Wind stress is zero as is surface heat fluxes (diurnal heating). ROMS onshore boundary (i.e., $x = 0$) is closed for all variables. At the offshore boundary, temperature is fixed to the initial conditions. The vertically varying cross-shore Eulerian mean velocity is set to anti-Stokes flow such that total offshore mass flux and heat flux is zero. Three simulations (denoted A, B, and C) are performed. Simulation A has stratification and TRCs through funwaveC coupling (Figure 1). Simulation B has stratification but no funwaveC coupling and thus no TRCs. Simulation C has TRCs but no stratification. A complete description of the modeling is provided elsewhere [*Kumar and Feddersen*, 2016a, 2016b].

In simulations A, B, and C, a conserved tracer is released in a near-bed ($z = -1.25$ m) alongshore strip ($0 < y < 1000$ m) within the surf zone at $x = -0.5L_{SZ} = -50$ m from $t = 0 - 2$ h and simulated for a total of 42 h. This conserved tracer can represent early-stage (passive) intertidal larvae or surf zone-released pollution. Prior to tracer release, the model is spun-up for 6 h. Surf zone overturning circulation and TRCs rapidly mix the tracer within the surf zone. Tracer releases farther offshore ($x = -100$m) yield similar results to those presented here (not shown). Tracer dilution D (e.g., Figures 1c and 1f) is defined as the tracer concentration

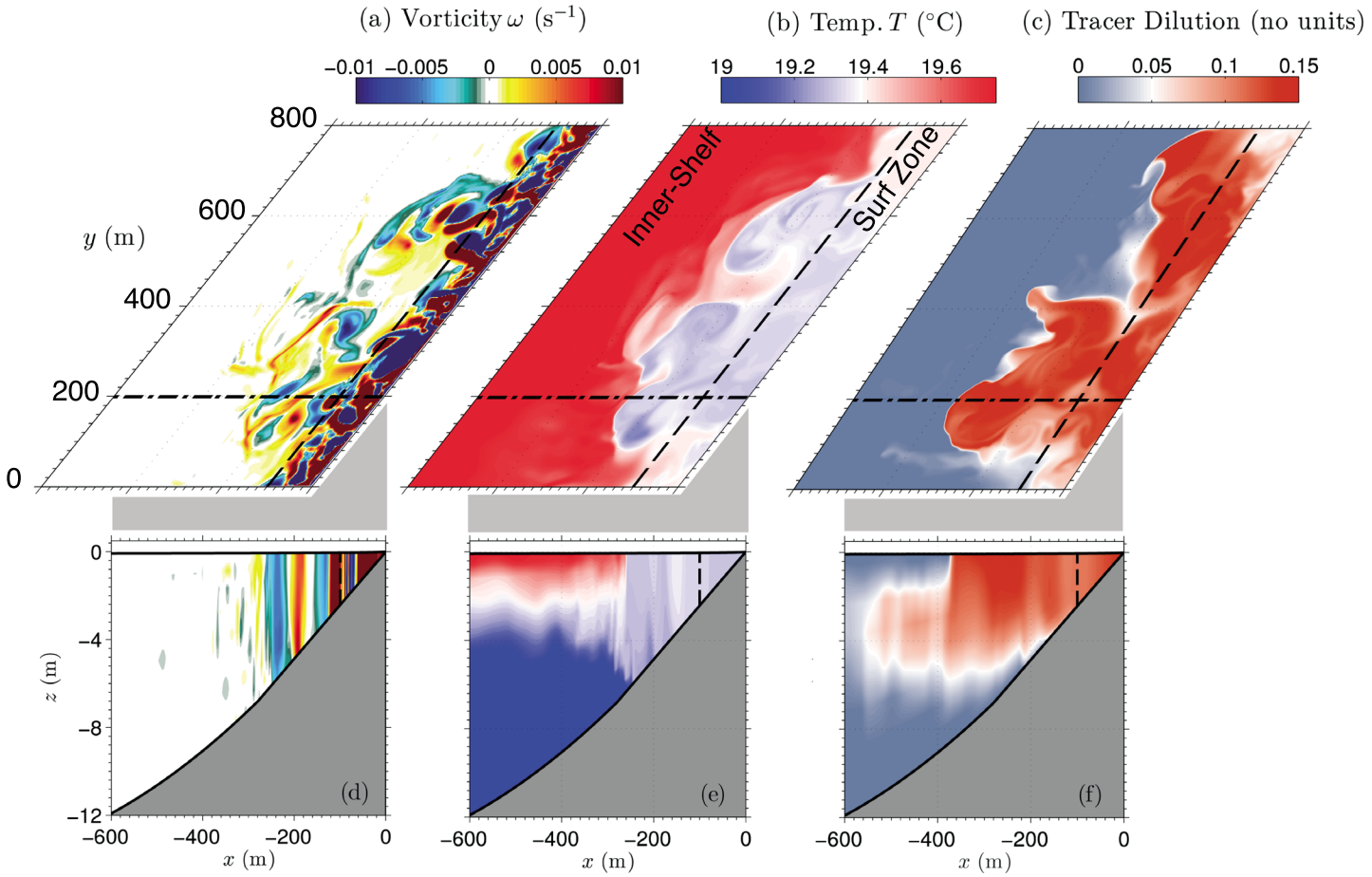

Figure 1. Snapshots of near-surface (a) vertical vorticity ω, (b) temperature T, and (c) tracer concentration versus cross-shore (x) and alongshore (y) coordinates at time t = 6 h. The surf zone (onshore of dashed line) has width L_{SZ} = 100 m, and the region offshore is the inner shelf. Below is a snapshot of cross-shelf transect of (d) vertical vorticity ω, (e) temperature T, and (f) tracer versus cross-shore (x) and vertical (z) coordinates at y = 200 m (dash-dotted line in Figures 1a–1c). Tracer was continuously released on an alongshore stripe at $x = -0.5L_{SZ} = -50$ m from 0–2 h. Transient rip currents bring surf zone tracer onto the inner shelf where it is subducted under the warmer inner-shelf water and advected offshore.

normalized by total tracer mass released divided by the surf zone volume. Diluted tracer time evolution is quantified with alongshore-averaged diluted tracer $\bar{D}(x, z)$ for simulations A–C.

3. Results

For simulation A (with TRCs and stratification) at t = 6 h (Figure 1), the surf zone has a rich eddy field [e.g., *Spydell and Feddersen*, 2009] and is vertically (z) well mixed in temperature and tracer due to strong breaking-wave turbulence [*Feddersen*, 2012]. Surf zone eddies coalesce and are cross shore (x) ejected as TRCs onto the inner shelf (Figures 1a and 1d). Within 300 m from shore, TRC-induced mixing leads to patchy near-surface cooling, depression of the T = 19°C isotherm, and stratification breakdown (Figures 1b and 1d). TRC export results in patchy tracer diluted to D = 0.15 out to within 300 m from shore with sharp surface tracer fronts. The region farther offshore (400–600 m from shore) is still stratified, with warm near-surface waters, and the T = 19°C isotherm slopes upward with undulations (Figures 1b and 1e). In this region (400–600 m from shore), near-surface tracer is zero (Figure 1c); however, tracer diluted to 0.1–0.05 is subducted and transported offshore in a subsurface layer between 2 and 5 m below the surface, representing a new offshore transport pathway.

From 6 h to 18 h after the release begins, the new offshore early-stage larval transport pathway brings most of the tracer subsurface and well offshore of the surf zone (Figure 2). Offshore transport in the subsurface layer is quantified with the time evolution of alongshore-averaged tracer dilution, $\bar{D}$, particularly the offshore propagation of the $\bar{D}$ = 0.05 front and the $\bar{D}$ maximum. When the tracer release ends (t = 2 h), the $\bar{D}$ = 0.05 front is at $x = -215$ m (Figure 2a) with weak tracer farther offshore. Onshore of the front, tracer is vertically well

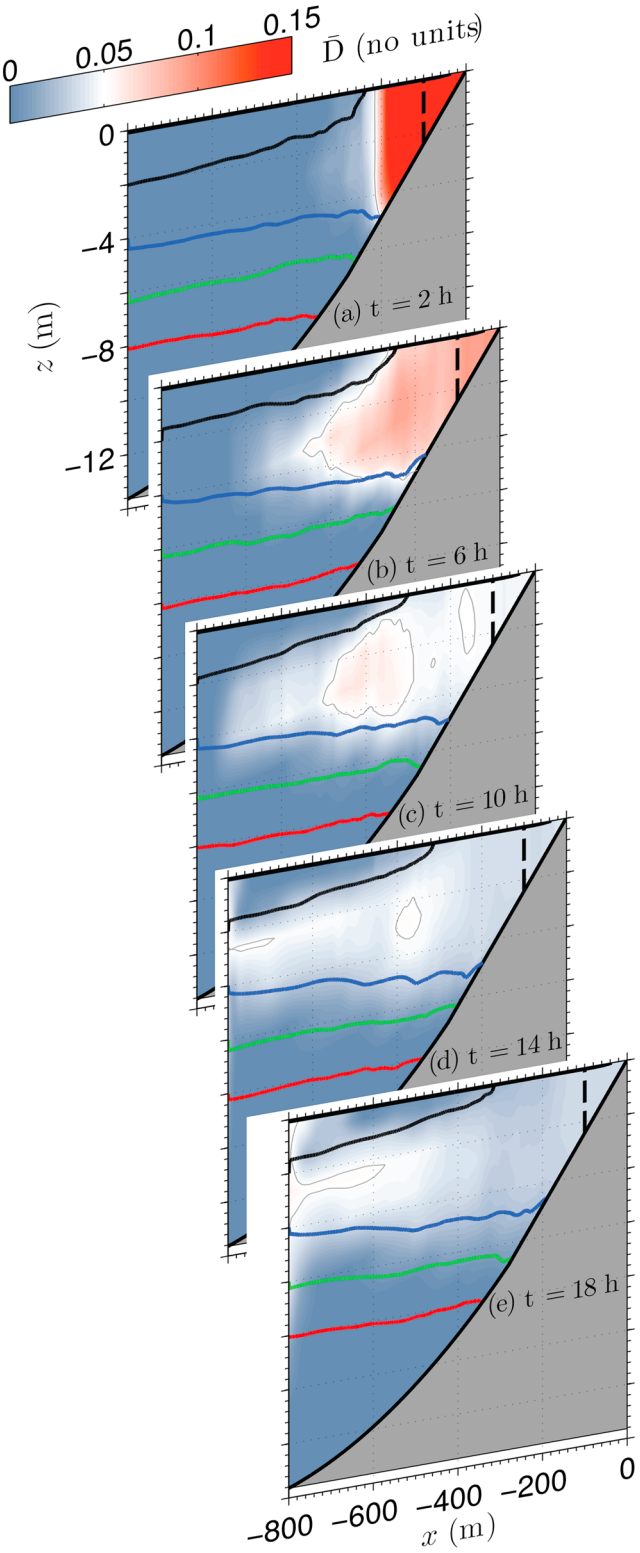

Figure 2. Simulation A (with TRCs and stratification) alongshore-averaged tracer dilution $\bar{D}(x, z)$ versus cross-shore (x) and vertical (z) coordinates at time (a) 2, (b) 6, (c) 10, (d) 14, and (e) 18 h from start of tracer release. The thin gray contour marks $\bar{D} = 0.05$. Solid red, green, blue, and black lines are alongshore averaged isotherms at 18, 18.5, 19, and 19.5 °C, respectively. The surf zone to inner-shelf boundary ($x = -L_{SZ}$) is indicated with the vertical dashed line, and tracer was released (from 0 to 2 h) at $x = -0.5L_{SZ} = -50$ m.

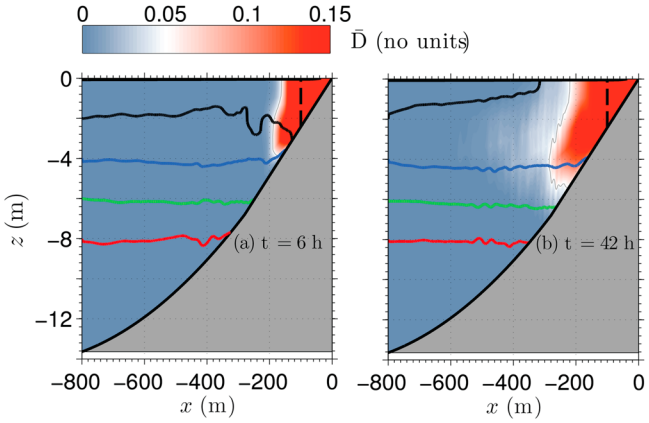

Figure 3. Simulation B (no TRCS, with stratification) alongshore-averaged tracer dilution $\bar{D}(x,z)$ versus cross-shore (x) and vertical (z) coordinates at time (a) $t = 6$ h and (b) 42 h. The thin gray contour denotes $\bar{D} = 0.05$. Solid red, green, blue, and black lines are alongshore-averaged 18, 18.5, 19, and 19.5°C isotherms. The surf zone to inner-shelf boundary ($x = -L_{SZ}$) is indicated with the vertical dashed line, and tracer was released (from 0 to 2 h) at $x = -0.5\ L_{SZ} = -50$ m.

mixed with surf zone maximum $\bar{D} = 0.32$. At $t = 6$ h, the near-surface $\bar{D} = 0.05$ front is still near $x = -240$ m, largely unchanged relative to $t = 2$ h. The maximum $\bar{D} = 0.1$ is still in the surf zone. However, the subsurface $\bar{D} = 0.05$ front reaches $x = -470$ m transporting tracer offshore between the strongly sloping 19.5°C and 19.0°C isotherms (Figure 2b). Over the next 12 h, nearly all tracer is transported offshore across the inner shelf between these 19–19.5°C isotherms (Figures 2c–2e), where stratification is a minimum. At $t = 10$ h, the subsurface tracer is transported even farther offshore almost reaching the offshore boundary (Figure 2c) as is the maximum $\bar{D} = 0.08$ at $x = -400$ m. With TRCs, the offshore transport of the $\bar{D} = 0.05$ front is 1.2 km/d. The vertical thickness of the diluted tracer reduces farther offshore (Figures 2c–2e) with the 19°C and 19.5°C isotherm narrowing. At $t = 18$ h, only 15% of the tracer is left in the onshore of $x = -200$ m and maximum $\bar{D}$ is far offshore near $x = -700$ m (Figure 2e). At $t = 14$ h and $t = 18$ h, $\bar{D}$ has encountered the offshore boundary ($x = -800$ m) limiting farther offshore transport (Figures 2d and 2e).

Most nearshore circulation models are wave averaged and do not include the mechanisms for generating TRCs [*Feddersen*, 2014]. Without TRCs but with stratification (simulation B), the alongshore-averaged diluted tracer $\bar{D}$ evolution has dramatically weaker offshore transport with most tracer staying within or near the surf zone (Figure 3). For example, at $t = 6$ h, the no-TRC $\bar{D} = 0.05$ front is near $x = -190$ m and tracer is strongly

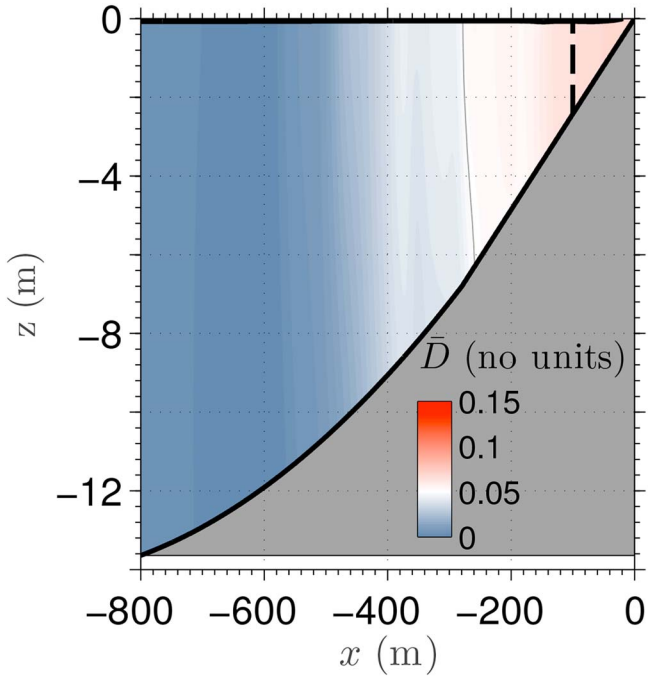

Figure 4. Simulation C (with TRCS, no stratification) alongshore-averaged tracer dilution $\bar{D}(x,z)$ versus cross-shore (x) and vertical (z) coordinates at time $t = 18$ h. The thin gray contour marks $\bar{D} = 0.05$. The surf zone to inner-shelf boundary ($x = -L_{SZ}$) is indicated with the vertical dashed line, and tracer was released (from 0 to 2 h) at $x = -0.5\ L_{SZ} = -50$ m.

concentrated in the surf zone with maximum $\bar{D} = 0.75$ (Figure 2). Even much later at $t = 42$ h, the no-TRC $\bar{D} = 0.05$ front is onshore of $x = -300$ m, the maximum $\bar{D} = 0.18$ is within the surf zone (Figure 3), and 59% of the tracer is still onshore of $x = -200$ m. Without TRCs, the $\bar{D}$ front is transported offshore at 0.06 km/d, only 5% of that with TRCs. Similar differences occur using the location of maximum $\bar{D}$. This demonstrates the important effect of TRCs in offshore transport across the stratified inner shelf particularly for early-stage larvae. Similarly, with TRCs and no stratification (simulation C) at $t = 18$ h, the $\bar{D} = 0.05$ front is at $x = -280$ m and maximum $\bar{D} = 0.07$ also is within the surf zone (Figure 4), in contrast to TRCs and stratification (Figure 2). In contrast to simulations A and B, simulation C $\bar{D}$ is largely vertically uniform. This demonstrates how this offshore transport pathway depends jointly upon stratification and TRCs.

4. Discussion and Conclusions

This new offshore transport pathway when TRCs and stratification are present (simulation A) is analogous to subduction at ocean fronts [e.g., *Rudnick and Luyten*, 1996], which has not been previously considered in nearshore contexts. This pathway is due to the following: First, TRCs, by eddy transport, bring surf zone tracer out to about $x = -300$ m (Figure 1). Vertical mixing associated with TRCs break down stratification onshore of $x = -300$ m, setting up a frontal structure with sloping isotherms farther offshore (Figure 2). At cross-shore locations farther offshore (i.e., $x < -300$ m), mixing is weak and the dynamics are largely geostrophic cross front and ageostrophic along front [*Kumar and Feddersen*, 2016b]. This cross-shore variation in turbulent mixing results in a cross-front secondary circulation [e.g., *Thompson*, 2000; *McWilliams et al.*, 2015] with near-surface onshore flow and offshore flow between the 19°C and 19.5°C isotherms (Figure 5). The offshore narrowing of these isotherms (Figures 2c–2e) may play a role in the formation of nearshore thin plankton layers [e.g., *Durham and Stocker*, 2012].

Between the 19°C and 19.5°C isotherms, stratification is minimum (Figure 6) as is the alongshore-averaged Ertel potential vorticity

$$\bar{q} = \rho_0^{-1}\left[\left(f + \frac{\partial \bar{v}}{\partial x}\right)\frac{\partial \bar{\rho}}{\partial z} - \frac{\partial \bar{v}}{\partial z}\frac{\partial \bar{\rho}}{\partial x}\right], \tag{1}$$

where $\bar{\rho}$ is the mean density derived from temperature and $\rho_0 = 1024\ \mathrm{kg\,m^{-3}}$. In the absence of mixing, $\bar{q}$ is also conserved, similar to the tracer. In simulation A, offshore mixing is weak and tongues of stratification and $\bar{q}$ minima are also subducted and transported offshore (Figure 6) by the secondary circulation as with the tracer (Figure 2). This is analogous to subduction under open ocean fronts on scales of 10 km [e.g., *Rudnick and Luyten*, 1996]. Offshore of $x < -400$ m, the planetary and relative vorticity terms contribute roughly equally to the stretching term in (1). This process is also analogous to the ongoing midwater column intrusion of a gravity current into a continuously stratified fluid [e.g., *Bolster et al.*, 2008]. However, direct comparison with scalings cannot be made as rotation is not included and adjustment of the density field is continuous with the recirculation pattern (Figure 5) which began 6 h prior to tracer release. The offshore model boundary at $x = -800$ m blocks farther offshore transport, and the net cross-shelf transport extent is uncertain. The cross-shelf width of the secondary circulation scales with the internal Rossby deformation radius L_D, which uses the initial stratification $N^2 = 6 \times 10^{-4}\ \mathrm{s^{-2}}$, and scale height of 6 m is $\approx$ 500 m. Thus, the secondary circulation is largely captured with this model domain. Without TRCs, vertical mixing just offshore of the surf zone is much weaker, as is the induced secondary circulation. This results in tracer (e.g., early-stage larvae) remaining close to shore ($x > -200$ m, Figure 3) and very little offshore transport.

TRCs are ubiquitous on all wave-exposed coasts, and the inner shelf is often stratified. Thus, this offshore transport pathway may be a dominant mechanism for export of early-stage invertebrate larvae. Properly modeling this offshore transport pathway will have implications for population connectivity and design of marine-protected areas. This mechanism also may play an important role in exporting harmful pathogens [*Boehm et al.*, 2015] or nutrients [*Halpern et al.*, 2012] which impact coastal water quality. Models that do not include TRCs and stratification will miss this subsurface offshore transport.

Over a range of beach slopes and normally incident wave heights, periods, and directional spreads, the TRC-induced barotropic (i.e., unstratified) mean exchange velocity is self-similar and significant out to $3L_{SZ}$ offshore [*Suanda and Feddersen*, 2015]. However, with stratification the rate of offshore tracer transport by this mechanism may depend upon these wave and beach slope parameters, which were fixed here. Similarly, the intensity of stratification (i.e., initial $\partial T/\partial z$) and its vertical variation likely also affect this offshore

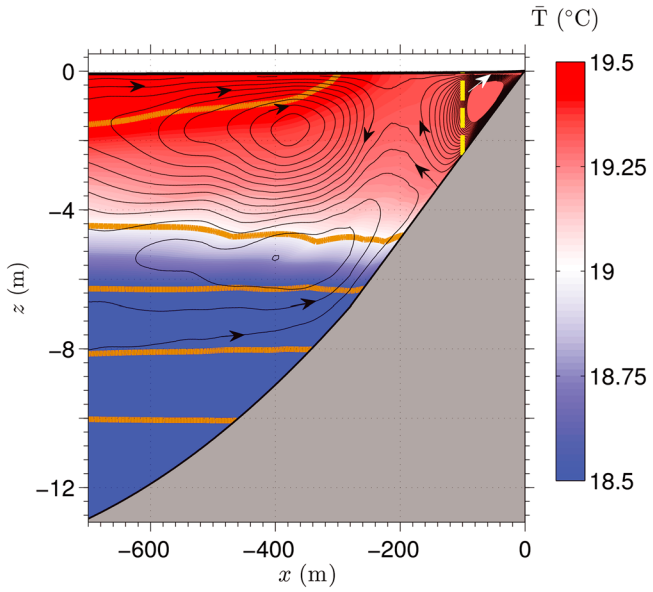

Figure 5. Mean Lagrangian (Eulerian + Stokes) stream function ψ_L (contour lines at 10^{-3} m^2 s^{-1} intervals) versus the cross-shore (x) and vertical (z) coordinates. Contours indicate direction of mean flow, and arrows show direction. Colored is the alongshore-averaged temperature $\bar{T}$ with solid dark yellow lines representing the 17.5, 18, 18.5, 19, and 19.5°C isotherms, respectively. The averaging is over 6–18 h and the alongshore. The dashed vertical yellow line delimits the surf zone $x = -L_{SZ}$.

transport mechanism. For example, if stratification began below the depth of the surf zone, this offshore transport mechanism may be suppressed. Other processes not considered here, like wind, diurnal heating and cooling, and internal tides which standard ocean circulation models resolve [e.g., *Kumar et al.*, 2015, 2016], may also be important on the inner shelf and interact with this transport mechanism.

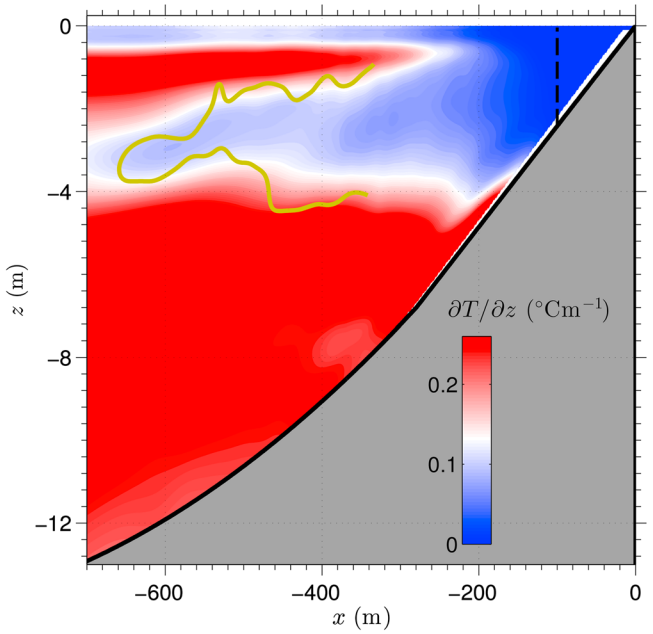

Figure 6. Simulation A (with TRCs and stratification) mean vertical temperature gradient $\partial\bar{T}/\partial z$ versus cross-shore (x) and vertical (z) coordinates averaged over the alongshore and 6–10 h after tracer release begins. The surf zone to inner-shelf boundary is indicated with the vertical dashed line. The Ertel potential vorticity (1) $\bar{q} = 2 \times 10^{-9}(ms)^{-1}$ contour (gold) outlines the tongue of minimum potential vorticity in the same 19–19.5°C layer where tracer is transported offshore.

Transient rip currents ejected onto a stratified inner shelf induce a new offshore transport pathway that subducts surf zone-origin tracers and transports them at least 800 m offshore at ≈1.2 km/d. This mechanism requires both TRCs and stratification and is analogous to subduction at ocean fronts. This mechanism may have an important role in exporting early-stage larvae, pathogens, or other tracers onto the shelf.

Acknowledgments
Funding support was provided by the Office of Naval Research. Melissa Omand, Peter Franks, and Ryan Rykaczewski provided useful comments. The authors declare that they have no competing financial interests. Model results from this study are available by contacting the corresponding author.

References

Austin, J. A., and S. J. Lentz (2002), The inner shelf response to wind-driven upwelling and downwelling, *J. Phys. Oceanogr.*, *32*(7), 2171–2193, doi:10.1175/1520-0485(2002)032<2171:TISRTW>2.0.CO;2.

Boehm, A. B. (2003), Model of microbial transport and inactivation in the surf zone and application to field measurements of total coliform in Northern Orange County, California, *Environ. Sci. Technol.*, *37*(24), 5511–5517, doi:10.1021/es034321x.

Boehm, A. B., N. S. Ismail, L. M. Sassoubre, and E. A. Andruszkiewicz (2015), Oceans in peril: Grand challenges in applied water quality research for the 21st century, *Environ. Eng. Sci.*

Bolster, D., A. Hang, and P. F. Linden (2008), The front speed of intrusions into a continuously stratified medium, *J. Fluid Mech.*, *594*, 369–377, doi:10.1017/S0022112007008993.

Booij, N., R. Ris, and L. H. Holthuijsen (1999), A third-generation wave model for coastal regions: 1. Model description and validation, *J. Geophys. Res.*, *104*(C4), 7649–7666.

Brown, J. A., J. H. MacMahan, A. J. H. M. Reniers, and E. B. Thornton (2015), Field observations of surf zone-inner shelf exchange on a rip-channeled beach, *J. Phys. Oceanogr.*, *45*, 2339–2355, doi:10.1175/JPO-D-14-0118.1.

Connolly, S. R., B. A. Menge, and J. Roughgarden (2001), A latitudinal gradient in recruitment of intertidal invertebrates in the northeast Pacific Ocean, *Ecology*, *82*(7), 1799–1813.

Cowen, R. K., and S. Sponaugle (2009), Larval dispersal and marine population connectivity, *Mar. Sci.*, *1*, 443–466.

Cowen, R. K., C. B. Paris, and A. Srinivasan (2006), Scaling of connectivity in marine populations, *Science*, *311*(5760), 522–527.

Durham, W. M., and R. Stocker (2012), Thin phytoplankton layers: Characteristics, mechanisms, and consequences, *Ann. Rev. Mar. Sci.*, *4*(1), 177–207, doi:10.1146/annurev-marine-120710-100957.

Feddersen, F. (2012), Scaling surf zone turbulence, *Geophys. Res. Lett.*, *39*, L18613, doi:10.1029/2012GL052970.

Feddersen, F. (2014), The generation of surfzone eddies in a strong alongshore current, *J. Phys. Oceanogr.*, *44*(2), 600–617.

Fujimura, A., A. Reniers, C. C. Paris, A. L. Shanks, J. MacMahan, and S. Morgan (2014), Numerical simulations of larval transport into a rip-channeled surf zone, *Limnol. Oceanogr.*, *59*, 1434–1447, doi:10.4319/lo.2014.59.4.1434.

Grant, S. B., J. H. Kim, B. H. Jones, S. A. Jenkins, J. Wasyl, and C. Cudaback (2005), Surf zone entrainment, along-shore transport, and human health implications of pollution from tidal outlets, *J. Geophys. Res.*, *110*, C10025, doi:10.1029/2004JC002401.

Hally-Rosendahl, K., and F. Feddersen (2016), Modeling surfzone to inner-shelf tracer exchange, *J. Geophys. Res. Oceans*, *121*, 4007–4025, doi:10.1002/2015JC011530.

Hally-Rosendahl, K., F. Feddersen, and R. T. Guza (2014), Cross-shore tracer exchange between the surfzone and inner-shelf, *J. Geophys. Res. Oceans*, *119*, 4367–4388, doi:10.1002/2013JC009722.

Hally-Rosendahl, K., F. Feddersen, D. B. Clark, and R. T. Guza (2015), Surfzone to inner-shelf exchange estimated from dye tracer balances, *J. Geophys. Res. Oceans*, *120*, 6289–6308, doi:10.1002/2015JC010844.

Halpern, B. S., et al. (2008), A global map of human impact on marine ecosystems, *Science*, *319*(5865), 948–952, doi:10.1126/science.1149345.

Halpern, B. S., et al. (2012), An index to assess the health and benefits of the global ocean, *Nature*, *488*(7413), 615–620, doi:10.1038/nature11397.

Kumar, N., and F. Feddersen (2016a), The effect of Stokes drift and transient rip currents on the inner-shelf. Part 1: No stratification, *J. Phys. Oceanogr.*, *47*, 227–241, doi:10.1175/JPO-D-16-0076.1.

Kumar, N., and F. Feddersen (2016b), The effect of Stokes drift and transient rip currents on the inner-shelf. Part 2: With stratification, *J. Phys. Oceanogr.*, *47*, 243–260, doi:10.1175/JPO-D-16-0077.1.

Kumar, N., G. Voulgaris, J. C. Warner, and M. Olabarrieta (2012), Implementation of the vortex force formalism in the coupled ocean-atmosphere-wave-sediment transport (COAWST) modeling system for inner shelf and surf zone applications, *Ocean Model.*, *47*, 65–95.

Kumar, N., F. Feddersen, Y. Uchiyama, J. McWilliams, and W. O'Reilly (2015), Midshelf to surfzone coupled ROMS-SWAN model data comparison of waves, currents, and temperature: Diagnosis of subtidal forcings and response, *J. Phys. Oceanogr.*, *45*(6), 1464–1490.

Kumar, N., F. Feddersen, S. Suanda, Y. Uchiyama, and J. McWilliams (2016), Mid-to inner-shelf coupled ROMS-SWAN model-data comparison of currents and temperature: Diurnal and semidiurnal variability, *J. Phys. Oceanogr.*, *46*(3), 841–862.

Lentz, S. J., and M. R. Fewings (2012), The wind- and wave-driven inner-shelf circulation, *Annu. Rev. Mar. Sci.*, *4*(1), 317–343, doi:10.1146/annurev-marine-120709-142745.

Luettich, R. A., J. L. Hench, C. W. Fulcher, F. E. Werner, B. O. Blanton, and J. H. Churchill (1999), Barotopic tidal and wind-driven larvae transport in the vicinity of a barrier island inlet, *Fish. Oceanogr.*, *8*(2), 190–209.

McWilliams, J. C., J. Gula, M. J. Molemaker, L. Renault, and A. F. Shchepetkin (2015), Filament frontogenesis by boundary layer turbulence, *J. Phys. Oceanogr.*, *45*(8), 1988–2005, doi:10.1175/JPO-D-14-0211.1.

Mullaney, T. J., and I. M. Suthers (2013), Entrainment and retention of the coastal larval fish assemblage by a short-lived, submesoscale, frontal eddy of the East Australian Current, *Limnol. Oceanogr*, *58*(5), 1546–1556.

Pineda, J. (1994), Internal tidal bores in the nearshore: Warm-water fronts, seaward gravity currents and the onshore transport of neustonic larvae, *J. Mar. Res.*, *52*(3), 427–458.

Pineda, J., J. A. Hare, and S. Sponaungle (2007), Larval transport and dispersal in the coastal ocean and consequences for population connectivity, *Oceanography*, *20*, 22–39, doi:10.5670/oceanog.2007.27.

Roughgarden, J., S. Gaines, and H. Possingham (1988), Recruitment dynamics in complex life cycles, *Science*, *241*, 1460–1466, doi:10.1126/science.11538249.

Rudnick, D. L., and J. R. Luyten (1996), Intensive surveys of the Azores front: 1. Tracers and dynamics, *J. Geophys. Res.*, *101*(C1), 923–939, doi:10.1029/95JC02867.

Scheltema, R. S. (1986), On dispersal and planktonic larvae of benthic invertebrates: An eclectic overview and summary of problems, *Bull. Mar. Sci.*, *39*(2), 290–322.

Shanks, A. L., and L. Brink (2005), Upwelling, downwelling, and cross-shelf transport of bivalve larvae: Test of a hypothesis, *Mar. Ecol. Prog. Ser.*, *302*, 1–12.

Shanks, A. L., and R. K. Shearman (2009), Paradigm lost? Cross-shelf distributions of intertidal invertebrate larvae are unaffected by upwelling or downwelling, *Mar. Ecol. Prog. Ser.*, *385*, 189–204.

Shanks, A. L., S. G. Morgan, J. MacMahan, and A. J. Reniers (2010), Surf zone physical and morphological regime as determinants of temporal and spatial variation in larval recruitment, *J. Exp. Mar. Biol. Ecol.*, *392*(1), 140–150, doi:10.1016/j.jembe.2010.04.018.

Shchepetkin, A. F., and J. C. McWilliams (2005), The regional oceanic modeling system (ROMS): A split-explicit, free-surface, topography-following-coordinate oceanic model, *Ocean Model.*, *9*(4), 347–404.

Siegel, D., S. Mitarai, C. Costello, S. Gaines, B. Kendall, R. Warner, and K. Winters (2008), The stochastic nature of larval connectivity among nearshore marine populations, *Proc. Natl. Acad. Sci. U.S.A.*, *105*(26), 8974–8979.

Spydell, M. S., and F. Feddersen (2009), Lagrangian drifter dispersion in the surf zone: Directionally spread, normally incident waves, *J. Phys. Oceanogr.*, *39*, 809–830.

Suanda, S. H., and F. Feddersen (2015), A self-similar scaling for cross-shelf exchange driven by transient rip currents, *Geophys. Res. Lett.*, *42*, 5427–5434, doi:10.1002/2015GL063944.

Thompson, L. (2000), Ekman layers and two-dimensional frontogenesis in the upper ocean, *J. Geophys. Res.*, *105*(C3), 6437–6451, doi:10.1029/1999JC900336.

Warner, J. C., B. Armstrong, R. He, and J. B. Zambon (2010), Development of a Coupled Ocean-Atmosphere-Wave-Sediment Transport (COAWST) modeling system, *Ocean Model.*, *35*(3), 230–244.

Werner, F. E., R. K. Cowen, and C. B. Paris-Limouzy (2007), Coupled biological and physical models, *Oceanography*, *20*(SPL. ISS. 3), 54–69.

Wong, S. H., A. E. Santoro, N. J. Nidzieko, J. L. Hench, and A. B. Boehm (2012), Coupled physical, chemical, and microbiological measurements suggest a connection between internal waves and surf zone water quality in the Southern California Bight, *Cont. Shelf Res.*, *34*, 64–78.